Cluster observations of a magnetic field cavity in the plasma sheet

N.C. Draper[a], M. Lester[a], S.W.H. Cowley[a], J.-M. Bosqued[b], A. Grocott[a], J.A. Wild[a], Y. Bogdanova[c], A.N. Fazakerley[c], J.A. Davies[d]

[a]*Radio and Space Plasma Physics Group, Department of Physics and Astronomy, University of Leicester, Leicester, LE1 7RH, UK;*
[b]*CESR/CNRS, BP 4346 9, Avenue Colonel Roche, 31028 Toulouse CEDEX 4, France;*
[c]*Mullard Space Science Laboratory, Holmbury St Mary, Dorking, Surrey, RH5 6NT, UK;*
[d]*Space Science and Technology Department, Rutherford Appleton Laboratory, Chilton, Didcot, Oxon, OX11 0QX, UK.*

Abstract

During the recovery phase of a substorm occurring on 1 September 2002 the four Cluster spacecraft crossed from the northern tail lobe into the plasma sheet. While the spacecraft were located in the plasma sheet boundary layer, the magnetic field data from the four spacecraft detected a cavity of close to zero magnetic field. The plasma in this cavity had characteristics similar to that of the central plasma sheet, possibly implying that the central plasma sheet expanded over the spacecraft. However, the unique four-spacecraft tetrahedral configuration of the Cluster spacecraft shows that this is not a valid scenario as the cavity passed over the four spacecraft, travelling continuously equatorwards and Earthwards. We present data from the Fluxgate Magnetometer, Cluster Ion Spectrometer, Plasma Electron and Current Experiment, and Research with Adaptive Particle Imaging Detectors instruments on board the Cluster spacecraft.

1. Introduction

The plasma sheet in the near-Earth tail is a region of closed field lines located in the equatorial region of the magnetotail. It is composed of the central plasma sheet and the plasma sheet boundary layer, which interfaces with the open field line of the tail lobes.

During summer 2002 the orbits of the Cluster spacecraft were optimized for data collection in the Earth's magnetotail, passing at regular intervals from the northern lobe, through the plasma sheet, and into the southern lobe. Their separation while in the magnetotail was consistently around 4,000 km. The tetrahedral formation of the spacecraft allows full temporal and spatial analysis of the data that are collected, revealing far more information than from a single spacecraft describing a similar orbit.

2. Instruments

The instruments used in this study are from the Cluster spacecraft: the Fluxgate Magnetometer (FGM; Balogh et al., 1997), the Cluster Ion Spectrometer (CIS; Rème et al., 1997, composed of the time-of-flight ion Composition and Distribution Function analyser (CODIF) and Hot Ion Analyser (HIA) instruments), the Plasma Electron and Current Experiment (PEACE; Johnstone et al., 1997), and the Research with Adaptive

Particle Imaging Detectors (RAPID; Wilken et al., 1997, from which the Imaging Electron Spectrometer (IES) instrument is used).

Data from the Tartu (Tar) station of the IMAGE ground magnetometer network (Viljanen and Häkkinen, 1997) are also presented. This station is located at 58.26° geographic latitude and 26.46° geographic longitude.

3. Data and Observations

Figure 1 shows the location of the Cluster spacecraft at 1900 UT on 1 September 2002 in the X-Z and X-Y planes in geocentric solar magnetospheric (GSM) coordinates. The relative locations of the spacecraft to each other are also shown on the right of each panel. Cluster 1 (Rumba) is blue, Cluster 2 (Salsa) is green, Cluster 3 (Samba) is yellow, and Cluster 4 (Tango) is red. The dotted lines depict model magnetic field lines using the Tsyganenko 1996 model (Tsyganenko and Stern, 1996). The spacecraft are located ~17 R_E downtail in the post-midnight sector, close to but northward of the equatorial plane. Cluster 3 is closest to the equatorial plane, with Cluster 4 furthest downtail and Cluster 2 closest to midnight.

Data from the Tartu station of the IMAGE magnetometer network (top two panels of Figure 2) indicate that at ~1900 UT the magnetosphere was in the recovery phase following a substorm that occurred at 1823 UT, detected as a decrease in the X component and evidence for Pi2 activity at onset. Much later, at 2305 UT, a second substorm was also detected.

Particle data from the Cluster instruments for 1800 to 2400 UT, also shown in Figure 2, indicate that during this interval the Cluster spacecraft were initially located in the lobe, passing through the plasma sheet boundary layer into the plasma sheet starting at 1903 UT. The CIS instrument on Cluster 4 (third and fourth panels of Figure 2) detects a sudden increase in ion density from ~0.01 cm^{-3} in the lobe to ~1 cm^{-3} in the plasma sheet, accompanied by velocity bursts to ~1,000 km s^{-1} in the V_x component (parallel to the magnetic field), which is typical of plasma sheet boundary layer beams. The PEACE and RAPID instruments on Cluster 4 also detect corresponding increases in the low- and high-energy electron fluxes, respectively. At the time of the second substorm, 2305 UT, the Cluster spacecraft re-entered the lobe due to the dipolarisation of the magnetotail at substorm expansion phase onset. For a more detailed analysis of these two substorms, see Draper et al. (2004).

Data from the FGM instruments on all four Cluster spacecraft for the interval 1900 - 1920 UT are shown in Figure 3. Around 1911 UT all components of the magnetic field decreased to close to zero nT, occurring in the order Cluster 4, Cluster 1, Cluster 2, and finally Cluster 3. Analysis of the spacecraft orientations relative to each other indicates that the field cavity was travelling Earthward, from dawn to dusk, and towards the equator (down on to the spacecraft). The magnetic field then recovered to a value of 16 nT (significantly less than the 29 nT detected before the magnetic field cavity) in the same order: 4,1,2,3. This indicates that the cavity passed completely over the spacecraft. The time taken for this was around 20 s; given the Cluster spacecraft separation of ~4,000 km indicates a velocity of the order of ~200 km s^{-1}. The scale size of the cavity is similar to that of the Cluster tetrahedron.

The CODIF and HIA data from the CIS instrument on Cluster 1 are shown for the interval 1900 - 1920 UT in Figure 4, with Cluster FGM data for comparison. The plasma sheet boundary layer beams are clearly seen as increased velocities (panel 3, CODIF and panel 5, HIA), high energy densities (panel 4, CODIF and panel 7, HIA) and increased temperature (panel 6, HIA). However, at ~1911 UT corresponding to the field cavity the velocities decreased to close to zero. This coincided with a high isotropic temperature (~5 keV) and enhanced energy density in the 1 to 10 keV energy range, detected at both the CODIF and HIA instruments.

Figure 5 shows distribution functions ($V_{parallel}$ against $V_{perpendicular}$) from the HIA instrument on Cluster 1 from 1904 to 1916 UT. The plasma sheet boundary layer beams were clearly seen from 1904 UT as enhanced fluxes in the $+V_{parallel}$ direction (towards Earth), with flux spread about zero $V_{perpendicular}$. From 1909 UT (before the magnetic cavity is detected by the FGM instrument) the distribution filled in in the $-V_{parallel}$ direction, from high pitch angles towards low, becoming gradually more isotropic. By 1911 UT the distribution was isotropic with very slow velocities, and looked like a typical central plasma sheet distribution. The distribution then returned to plasma sheet boundary layer beams, with evidence for mirrored particles, as flux was detected in the $-V_{parallel}$ direction. From 1915 UT the spacecraft entered the central plasma sheet, detecting an isotropic distribution function. A similar series of distribution functions was detected by the Cluster 3 HIA instrument (data not shown), delayed by ~40 s with respect to Cluster 1. This is as expected, since Cluster 3 was the last of the four spacecraft to be passed over by the cavity.

4. Discussion

The Cluster spacecraft detected a magnetic cavity at 1911 UT on 1 September 2002 when crossing from the northern lobe of the magnetotail into the plasma sheet during the recovery phase of a magnetospheric substorm. This cavity was clearly embedded within the plasma sheet boundary layer, and associated with the plasma sheet boundary layer crossing. It was moving Earthwards, from dawn to dusk and equatorward over the spacecraft, travelling at ~200 km s^{-1}, and was filled with hot, dense, isotropic, low velocity plasma. Its characteristics were similar to that of the central plasma sheet. However, the FGM data from the four separate Cluster spacecraft indicate that this cavity could not have been the central plasma sheet as it was clearly associated with the plasma sheet boundary layer, and not travelling in a direction indicative of the central plasma sheet expanding and contracting over the spacecraft.

Further study of this unusual plasma sheet boundary layer magnetic cavity is required to accurately determine its characteristics and origin. This is not a solitary event; another similar cavity is detected later on the same day, also during the recovery phase of a magnetospheric substorm. Further potential magnetic cavity candidates have also been identified for inclusion in a statistical survey of these interesting new structures.

Figures

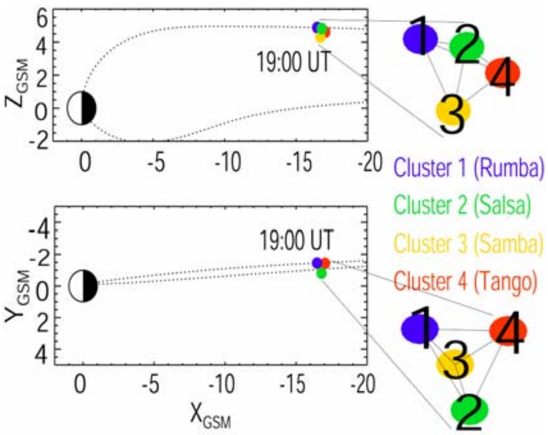

Figure 1

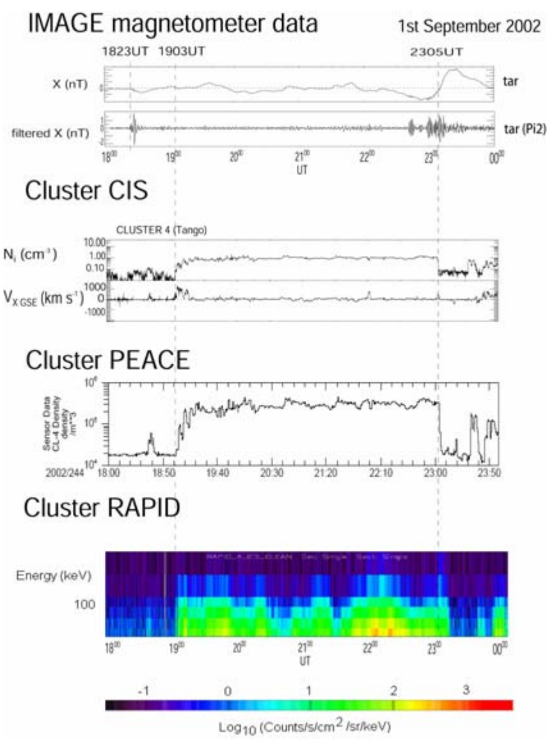

Figure 2

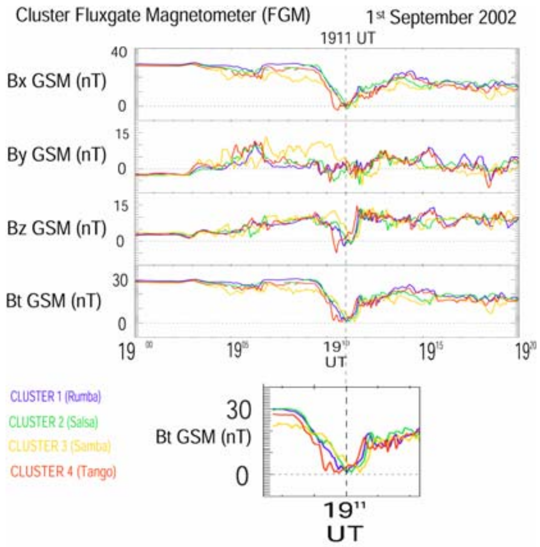

Figure 3

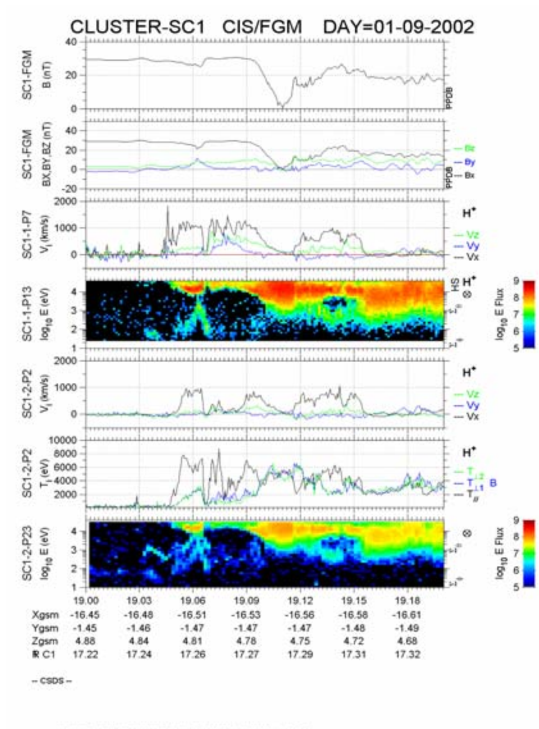

Figure 4

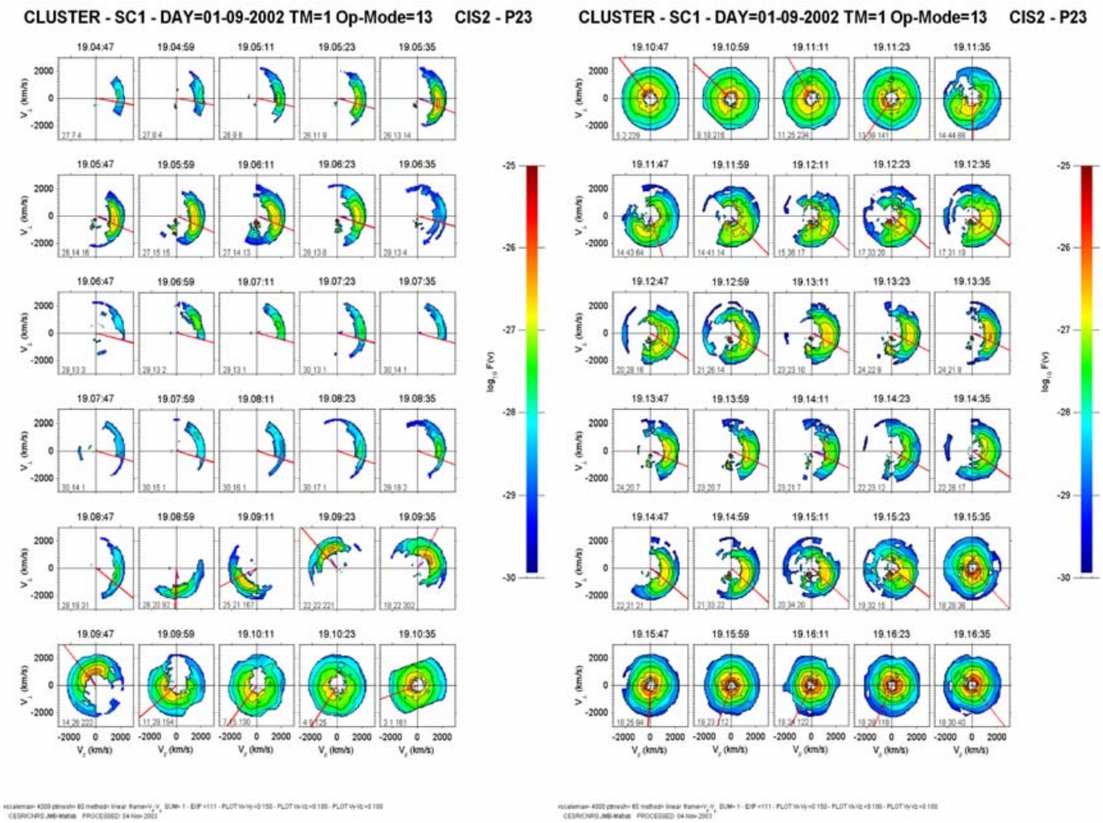

Figure 5

References

Balogh, A., Dunlop, M.W., Cowley, S.W.H. et al., The Cluster magnetic fields investigation. Space Sci. Rev., 79, 65-91, 1997.

Draper, N.C., Lester, M., Wild, J.A. et al., A joint Cluster and ground-based instruments study of two magnetospheric substorm events on 1st September 2002. Submitted to Ann. Geophys., 2004.

Johnstone, A.D., Alsop, C., Burge, S. et al., Peace: A Plasma Electron and Current Experiment. Space Sci. Rev., 79, 351-398, 1997.

Rème, H., Bosqued, J.-M., Sauvaud, J.A. et al., The Cluster Ion Spectrometry (CIS) Experiment. Space Sci. Rev., 79, 303-350, 1997.

Tsyganenko, N.A. and Stern, D.P., Modeling the global magnetic field of the large-scale Birkeland current systems, J. Geophys. Res., 101, 27187-27198, 1996.

Viljanen, A. and Häkkinen, L., IMAGE magnetometer network. In: Satellite-Ground Based Coordination Sourcebook (Ed. M. Lockwood, M.N. Wild and H.J. Opgenoorth), ESA publications SP-1198, p. 111-117, 1997

Wilken, B., Axford, W.I., Daglis, I. et al., RAPID. The Imaging Energetic Particle Spectrometer on Cluster. Space Sci. Rev., 79, 399-473, 1997.

Figure captions

Figure 1: Cluster spacecraft positions at 1900 UT on 1 September 2002, shown projected into the X-Z and X-Y planes in geocentric solar magnetospheric (GSM) coordinates, with the relative orientation of the spacecraft in each plane to the right of

each panel. Blue represents Cluster 1 (Rumba), green Cluster 2 (Salsa), yellow Cluster 3 (Samba) and red Cluster 4 (Tango). Dotted lines depict the model magnetic field.

Figure 2: IMAGE magnetometer data and Cluster particle data for 1 September 2002 (1800 to 2400 UT). Top two panels show the X component of magnetic field at the Tartu (Tar) IMAGE magnetometer station, and the filtered X component at the same station (filter range is in the period band 20 - 200 s). The third and fourth panels show the density and x component of velocity of the low-energy ions (0.02 eV to 30 keV) from the CIS instrument on the Cluster 4 spacecraft. The fifth panel shows the density of the low-energy electrons (0.7 eV to 30 keV) from the PEACE instrument on the Cluster 4 spacecraft. The sixth panel shows the electron density of the high-energy electrons (20 to 400 keV) from the RAPID IES instrument on the Cluster 4 spacecraft.

Figure 3: Cluster FGM data for 1 September 2002 for the interval 1900 - 1920 UT. The B_x, B_y and B_z components and the total magnetic field are shown in GSM coordinates. The total field strength is shown on an expanded scale at the bottom of the Figure centred on the field null at ~1911 UT.

Figure 4: FGM and CIS data for 1 September 2002 for the same interval as Figure 2 (1900 - 1920 UT). Panels show from top to bottom, the total magnetic field and B_x, B_y and B_z magnetic field components, the velocity components and energy density for CIS1 (CODIF) and the velocity, temperature and energy density for CIS2 (HIA).

Figure 5: Cluster 1 CIS2 (HIA) distribution functions for 1 September 2002 for 1904 to 1916 UT, at 12 s intervals (read left to right and top to bottom across left page first, then right page). Each panel shows $V_{parallel}$ against $V_{perpendicular}$; the red line depicts the sun direction.